

Improved Color Barycenter Model for Road-Sign Detection

Qieshi Zhang and Sei-ichiro Kamata
 Graduate School of Information, Production and Systems
 Waseda University, Japan.

Q.Zhang@Akane.Waseda.jp, Kam@Waseda.jp

Abstract

This paper proposes an improved color barycenter model (CBM) for road sign detection. The previous version of CBM can find out the colors of road-sign (RS), but its accuracy is not high enough for magenta and blue region segmentation. The improved CBM extends the barycenter distribution to cylinder coordinate and takes the number of colors in every point into account. Then the K-means clustering is used to analyze the distribution under cylinder coordinate. Using Geodesic distance instead of Euclidean distance for K-means clustering and some conditions provided by the initial color region of CBM is used to constrain K-means operation. The experimental results show that the improved method is able to detect RS with high robustness.

1 Introduction

The research of road-sign (RS) detection becomes important for driver navigation, recently. Because it can regulate traffic and indicate road situations for guidance and warning. The detection of RS is important in driver assistance system (DAS). For example, if drivers disregard the temporary stop sign or the speed-limit sign, accidents may happen. The framework of DAS was first introduced by Arnoul *et al.* [1], which gives the required functions of DAS. Although the DAS is a good way to avoid much neglect, the detection of RS is not easy from videos directly, due to the unknown changes of driving environment conditions.

Many researchers have been devoted themselves to solve this problem [2] by considering the RS with stronger features, such as high contrast, bright colors and fixed shapes. In recently years, the color based methods become popular, some of these methods are desired under different color spaces, in which RGB space is widely used. Based on this color space, Estevez and Kehtarnavaz [3] threshold the redness pixels by the difference of R with the connection of G & B . Fang *et al.* [4] use the Neural Network (NN) to extract the color and shape feature in RGB color space. After that, Zhang *et al.* [5][6] propose original color barycenter model (CBM) and analyze the barycenter distribution in hexagon region to analyze the color feature through the RGB color space conversion. Another most frequently employed space is HSI. Liu *et al.* [7] present a pseudo RGB-HSI conversion method without nonlinear transform to extract different color. Beside the RGB and HSI space, HSV [8], HLS [9], YIQ [10] and YUV [11] are also be used for RS detection.

However, these kinds of methods are sensitive to the lighting condition. Moreover, the existing color analysis based methods only try to find one component of 3D color space and segment it. In this paper, to over-

come the limitations of the existing color space based methods and detect the color feature more effectively, the original CBM is extended to cylinder coordinate for acquiring more accurate segmentation result.

2 Proposed Method

Although the barycenter distribution of CBM in rectangular coordinate system (RCS) can be used in different conditions by the segmentation strategy [5][6], it ignores to analyze the influence of the number of barycenter in same positions. Fig. 1 shows an example of real scene and its corresponding barycenter distribution in polar coordinates system (PCS) and RCS, respectively. Fig. 1(d) shows the result separated by seven regions as M (Magenta), R (Red), Y (Yellow), G (Green), C (Cyan), B (Blue), and L (Luminance). Considering the characteristic of the barycenter distribution and K-means clustering, the constrained K-means clustering method is studied to clustering the barycenter distribution to replace the curve based linear segmentation [Fig.1(c)].

2.1 CBM Extension — Cylinder Coordinate

In this subsection, the CBM is extended to cylinder coordinate from PCS to overcome the shortage of original model [5] by following steps.

1. Create color triangle as [5] described by converting the RGB color space into three 2D points and connect them. The coordinates of three color apexes are:

$$\begin{cases} (R_x, R_y) = (0, R_v) \\ (G_x, G_y) = \left(-\frac{\sqrt{3}G_v}{2}, -\frac{G_v}{2}\right) \\ (B_x, B_y) = \left(\frac{\sqrt{3}B_v}{2}, -\frac{B_v}{2}\right) \end{cases}, \quad (1)$$

where the R_v , G_v , and B_v are the original value of pixel color.

2. Define the coordinate of color barycenter (C_x , C_y) as Eq. (2):

$$\begin{cases} C_x = \frac{1}{3}(R_x + G_x + B_x) \\ C_y = \frac{1}{3}(R_y + G_y + B_y) \end{cases}. \quad (2)$$

3. Calculate all barycenters of image and describe them in a hexagon region in PCS as shown in Fig. 1(a).
4. Expand the distribution from the origin in PCS into RCS as shown in Fig. 1(c). In the RCS, the coordinate of color barycenter is converted from (C_x , C_y) to (φ , r):

$$\begin{cases} \varphi = C_y/C_x \\ r = \sqrt{C_x^2 + C_y^2} \end{cases}, \quad (3)$$

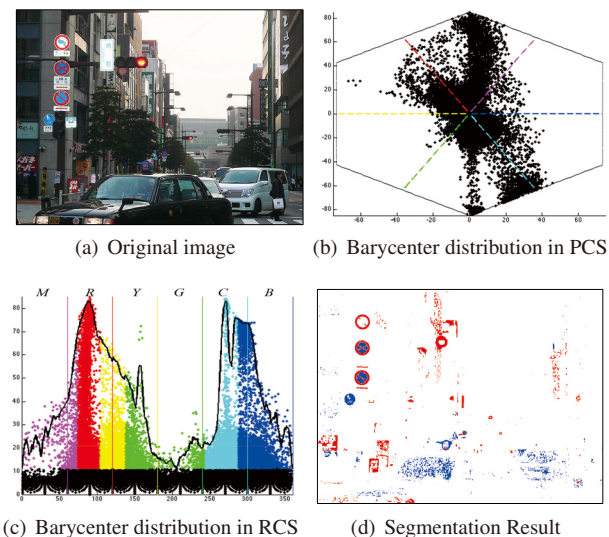


Figure 1. The barycenter distribution of original color barycenter model [5][6].

- Roll up the distribution in 2D RCS to cylinder to create the cylinder coordinate system (CCS), in order to connect all color regions continuous. The coordinate in CCS is (x, y, z) , which is calculated by (φ, r) :

$$\begin{cases} x = \sin(\varphi) \\ y = \cos(\varphi) \\ z = r \end{cases}, \quad (4)$$

where φ and r indicate the offset and intensity of color, the radius of cylinder is set to 1. Based on this conversion, all the barycenters are converted into the surface of cylinder as shown in Fig. 2(d).

After these steps, the distribution of color barycenter is converted onto surface of cylinder to keep the relation of color more accurately. Then, considering the influence of number of every barycenter, the constrained K -means is studied to cluster the color barycenters into seven clusters for segmentation.

2.2 CBM Distribution Constrained K -means

In this paper, the prior knowledge of color distribution region is used as the constraint. The colors should be separated into 7 regions, one is the gray region (L) to show the achromatic information, and the other 6 regions are the color region to show different major colors. In practical, the captured color of RS usually has little offset with real color because of the various environments or different capture device, so it will offset in the boundary region with $\pi/12$ of corresponding color region.

In our constrained K -means algorithm, all the barycenters are on the surface of the cylinder, so the Euclidean distance is not suitable here. Here, we assume the cylinder surface is a low dimension Manifold, and define the Geodesic distance in the surface. By observing the characteristic of the cylinder surface, the distance should be the arc from point p to q as the red curve shown in Fig. 2(c). Consider the point coordinate in the CCS is (x, y, z) , so the Geodesic distance

is defined as Eq. (5):

$$G_dis(p, q) = \sqrt{|z_p - z_q|^2 + arc_{2D}^2(p_{2D}, q_{2D})}, \quad (5)$$

where arc_{2D} is the length of arc from points p_{2D} to q_{2D} in the circle of undersurface as the orange curve shown in Fig. 2(c) which calculated by Eq. (6):

$$arc_{2D}(p_{2D}, q_{2D}) = \left| \arctan\left(\frac{y_p}{x_p}\right) - \arctan\left(\frac{y_q}{x_q}\right) \right|. \quad (6)$$

Here, the initial region Reg_k of all clusters is defined as:

$$Reg_k = \begin{cases} x = \sin(\varphi), & \varphi_{k-1} < \varphi < \varphi_k; \\ y = \cos(\varphi), & \varphi_{k-1} < \varphi < \varphi_k; \\ z = r, & 0 \leq r \leq 85. \end{cases} \quad (7)$$

In the Eq. (7), the $k \in K$ is the index of current cluster, φ_{k-1} and φ_k are the boundary of Reg_k . In this paper, φ_k is set by $\{\varphi_{MR} < \varphi_{RY} < \varphi_{YG} < \varphi_{GC} < \varphi_{CB} < \varphi_{BM}\}$, which defined in above section. The pseudocode of this procedure is given in Algorithm (1).

Based on the improvement of constraint with the cylinder coordinate of color barycenter distribution, the clustered result is shown in Fig. 2(d) and the obtained segmentation result is shown in Fig. 2(e). Fig. 2(a) and (b) are the cluster result in PCS and RCS, respectively. These results show the performance of the constrained K -means. Comparing the segmentation result of improved CBM [Fig. 2(d)] with the barycenter distribution in RCS and in PCS [5] [Fig. 1(c)], the improved CBM can obtain more accurate result.

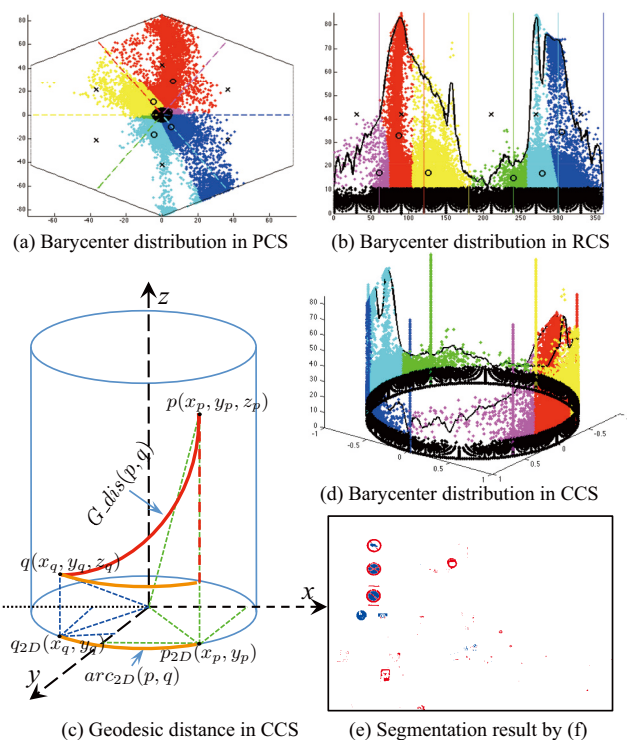


Figure 2. Color barycenter distribution in PCS, RCS, CCS and segmentation result of Fig. 1(a).

Algorithm 1 Constrained K -means Algorithm.

Input:

$\mathbf{X} = \{\mathbf{x}_1, \dots, \mathbf{x}_N\} \in \mathbb{R}^D$ ($N \times D$ input data set),
 $\mathbf{C} = \{\mathbf{c}_1, \dots, \mathbf{c}_K\} \in \mathbb{R}^D$ (K cluster centers).

- 1: Cluster centers $\mathbf{C} \in \mathbf{X}$ initialization: calculate the geometric center \mathbf{c}_k of the default color region \mathbf{R}_k as the initial cluster centers.
- 2: **while** *termination criterion is not met* **do**
- 3: **for** ($i = 1; i \leq N; i = i + 1$) **do**
- 4: Assign \mathbf{x}_i to the nearest cluster;
- 5: $m[i] = \arg \min_{k \in \{1, \dots, K\}} G_dis(\mathbf{x}_i - \mathbf{c}_k)$, Eq. (5);
- 6: **end for**
- 7: Recalculate the cluster centers;
- 8: **for** ($k = 1; k \leq K; k = k + 1$) **do**
- 9: Cluster S_k contains the set of points \mathbf{x}_i that are nearest to the center \mathbf{c}_k :
- 10: $S_k = \{\mathbf{x}_i | m[i] = k\}$;
- 11: Calculate new center \mathbf{c}_k as the mean of points that belong to S_k :
- 12: $\mathbf{c}_k = \frac{1}{|S_k|} \sum_{\mathbf{x}_i \in S_k} \mathbf{x}_i$;
- 13: Judge if the current cluster center \mathbf{c}_k in the corresponding region \mathbf{R}_k :
- 14: **if** $\mathbf{c}_k \notin \mathbf{R}_k$ **then**
- 15: **if** $\varphi_{c_k} < \varphi_{k-1}$ **then**
- 16: $x_{c_k} = \sin(\varphi_{k-1})$;
- 17: $y_{c_k} = \cos(\varphi_{k-1})$;
- 18: **end if**
- 19: **if** $\varphi_{c_k} > \varphi_k$ **then**
- 20: $x_{c_k} = \sin(\varphi_k)$;
- 21: $y_{c_k} = \cos(\varphi_k)$;
- 22: **end if**
- 23: **else**
- 24: continue;
- 25: **end if**
- 26: **end for**
- 27: **end while**

Output:

$\mathbf{C} = \{\mathbf{c}_1, \dots, \mathbf{c}_K\} \in \mathbb{R}^D$ (K cluster centers),
 $\text{Idx} = \{\text{id}x_1, \dots, \text{id}x_N\} \in \mathbb{R}^D$ ($N \times D$ output index set).

3 Experimental and Discussion

3.1 RS Candidates Extraction

Based on the above strategy to separate the color region of RS, the RS candidates can be detected. After that, some simple geometric property based filtering is used. As the RS can be circular, rectangular or triangular, the following three criteria are used to filter out the impossible candidates:

1. The first criterion is size of RS. It requires the area of RS candidates in the range as Eq. (8)

$$A_{min} W_{RS} H_{RS} < Area_{RS} < A_{max} W_{RS} H_{RS}, \quad (8)$$

where $Area_{RS}$ is the area of RS candidate. W_{RS} and H_{RS} are the width and height of RS, respectively. By analyzing several different sizes of RS in the test video (640×480), we have found that if the

candidate size is smaller than 12×12 pixels, it is difficult to be observed. And no matter how long the distance is, the size of RS cannot be larger than 50×50 pixels, so the minimum size coefficient A_{min} set as 0.0005 and maximum size coefficient A_{max} set as 0.008.

2. The second criterion is aspect ratio. It requires the RS candidates to satisfy the ratio as:

$$\min\left(\frac{H_{RS}}{W_{RS}}, \frac{W_{RS}}{H_{RS}}\right) > AR, \quad (9)$$

which AR is the aspect ratio, and for circular, rectangular, and triangular the ideal ratio is $AR = 1$, but in fact it always has some shift. For deciding AR threshold, we select 50 detected RS random and get the statistics to set AR as 0.86. As a result, the noises and some wrong candidates have been eliminated. However, some regions, which have the same size and shape of real RS are selected by mistake. So to remove these wrong candidates, the color ratio is necessary.

3. The third criterion is color ratio. To decide the color ratio, we calculate the color percentage in the standard RS block. Based on the color ratio, we consider the influence of colorcast and fade, and let the error with 15% of standard RS be accepted. If one of the criteria is satisfied, it will be accepted by the following color percentage: Red $\in [31.6\%, 65.1\%]$, Blue $\in [20.9\%, 68.5\%]$, and Yellow $\in [23.4\%, 45.8\%]$.

After filtering by these criteria, the final detection result can be obtained. More examples and comparisons are described in experiment.

3.2 Experimental Results and Discussion

In this section, several experiments are given to verify the efficiency and robustness of the proposed method. For evaluating the results, the accuracy and the detected results with other methods are compared.

In this experiment, the results indicate that the proposed method can be used to detect RS in blurred and weak light conditions. Fig. 3 shows an example in sunny and Figs. 4 and 5 show the detection results with a signal and two signs in real situations (different size/distance in one scene). In these figures, some reference methods are used for comparison, and the results are shown in Table 1. Results show that the proposed method is robust under different size and light.

4 Conclusion

In this paper, the cylinder expression based extension of the original CBM is presented. And the constrained K -means is proposed to segment the CBM cylinder distribution for RS detection. The improved segmentation strategy can overcome the shortage of existing color analysis based method. And the experimental results show that the proposed method achieve good performance under different environments.

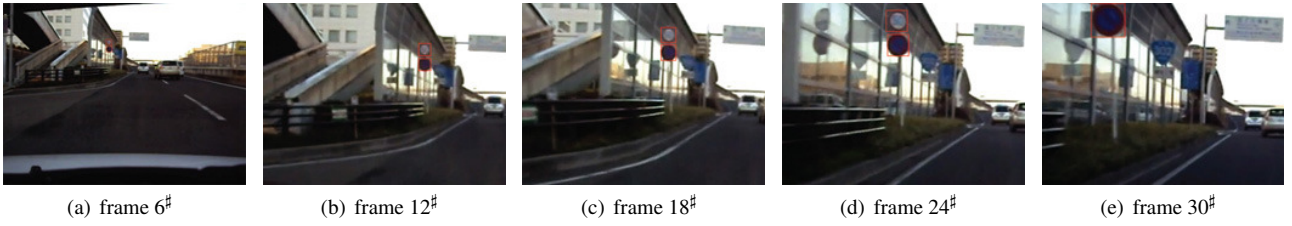


Figure 3. RS detection in sunny, 640×480 , 15 fps, 32 frames.

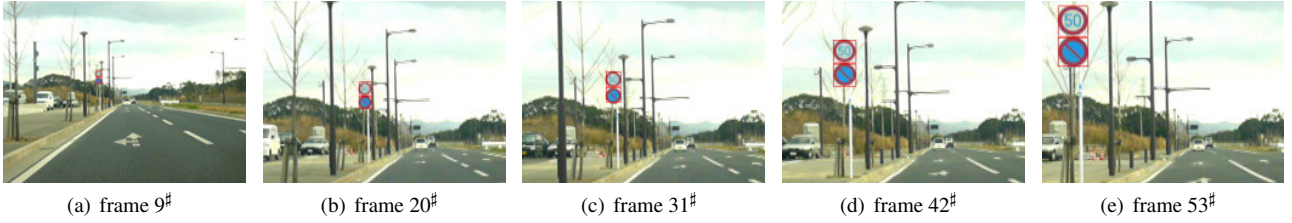


Figure 4. RS detection for multiply signs, 640×480 , 15 fps, 55 frames.

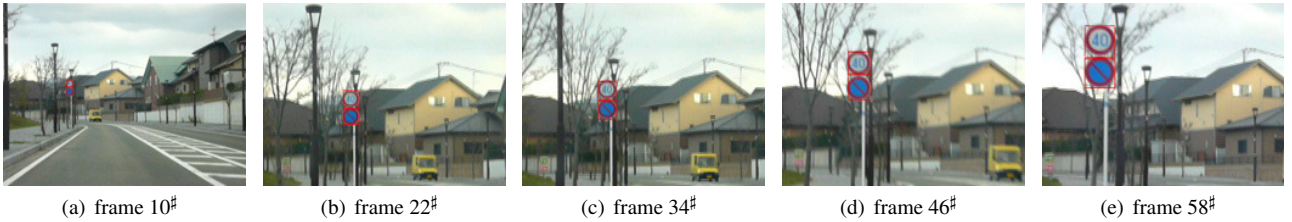


Figure 5. RS detection for multiply signs, 640×480 , 15 fps, 60 frames.

Table 1. Detection Results (640×480 , 15 fps, 12 video sequences, 631 frames with 1012 RS).

No.	Proposed	Reference [5]	Reference [10]	Reference [12]	Reference [13]	Reference [14]
Detected	953 (94.2%)	848 (83.8%)	706 (69.8%)	797 (78.8%)	830 (82.0%)	852 (84.9%)
Wrong detected	61 (6.0%)	82 (8.1%)	136 (13.4%)	124 (12.3%)	119 (11.8%)	120 (11.9%)
Not detected	103 (10.2%)	204 (16.2%)	306 (16.2%)	215 (21.2%)	182 (18.0%)	170 (15.8%)

References

- [1] P. Arnoul, M. Viala, J. Guerin, and M. Mergy, "Traffic signs localisation for highways inventory from a video camera on board a moving collection van," *IEEE IV*, pp.141–146, 1996.
- [2] V. Kastinaki, M. Zervakis, and K. Kalaitozakis, "A survey of video processing techniques for traffic applications," *Image and Vision Computing*, vol.21, no.4, pp.359–381, 2003.
- [3] L. Estevez and N. Kehtarnavaz, "A real-time histogram approach to road sign recognition," *Proc. of the IEEE Southwest Symp. on Image Analysis and Interpretation*, pp.95–100, 1996.
- [4] C.Y. Fang, S.W. Chen, and C.S. Fuh, "Road-sign detection and tracking," *IEEE TVT*, vol.52, no.5, pp.1329–1341, 2003.
- [5] Q. Zhang and S. Kamata, "Automatic road sign detection method based on color barycenters hexagon model," *ICPR*, pp.1–4, 2008.
- [6] Q. Zhang and S. Kamata, "A novel color descriptor for road-sign detection," *IEICE T Fund. Electr.*, vol.E96-A, no.5, 2013.
- [7] W. Liu, X. Chen, B. Duan, H. Dong, P. Fu, H. Tuan, and H. Zhao, "A system for road sign detection, recognition and tracking based on multi-cues hybrid," *IEEE IV*, pp.562–567, 2009.
- [8] S. Vitabile, G. Pollaccia, G. Pilato, and E. Sorbello, "Road signs recognition using a dynamic pixel aggregation technique in the hsv color space," *IEEE ICIAP*, pp.572–577, 2001.
- [9] H. Fleyeh, "Color detection and segmentation for road and traffic signs," *CIS*, vol.2, pp.809–814, 2004.
- [10] N. Kehtarnavaz and A. Ahmad, "Traffic sign recognition in noisy outdoor scenes," *IEEE IV*, pp.460–465, 1995.
- [11] J. Miura, T. Kanda, and Y. Shirai, "An active vision system for real-time traffic sign recognition," *IEEE ITS*, pp.52–57, 2000.
- [12] A. de la Escalera, L.E. Moreno, M.A. Salichs, and J.M. Armingol, "Road traffic sign detection and classification," *IEEE TIE*, vol.44, no.6, pp.848–859, 1997.
- [13] L.W. Tsai, J.W. Hsieh, C.H. Chuang, Y.J. Tseng, K.C. Fan, and C.C. Lee, "Road sign detection using eigen colour," *IET Computer Vision*, vol.2, no.3, pp.164–177, 2008.
- [14] S. Maldonado-Bascon, S. Lafuente-Arroyo, P. Gil-Jimenez, H. Gomez-Moreno, and F. Lopez-Ferreras, "Road-sign detection and recognition based on support vector machines," *IEEE TITS*, vol.8, no.2, pp.264–278, 2007.